Colloid Polym Sci 278:682–686 (2000)


SHORT COMMUNICATION

S.-Y. Zhao
S.-B. Lei
S.-H. Chen
H.-Y. Ma
S.-Y. Wang

# Assembly of two-dimensional ordered monolayers of nanoparticles by electrophoretic deposition

Received: 7 October 1999
Accepted: 25 January 2000

S.-Y. Zhao · S.-B. Lei · S.-H. Chen (✉)
H.-Y. Ma
Department of Chemistry
Shandong University
Jinan 250100, China
e-mail: shchen@public.sdu.edu.cn

S.-Y. Wang
Testing Center of Shandong Teachers' University, Jinan 250014, China

**Abstract** In this article the effect of field strength, temperature and square-wave pulse on the deposition structure of gold nanoparticles is investigated and 2D structures of silver and two kinds of rare-earth carbonate particles are synthesized by electrophoretic deposition (EPD). The results indicate that EPD is a general phenomenon that occurs on the electrode/sol interface and that the EPD method may be developed for the assembling of 2D structures of nanoparticles. On the other hand, the results also show that the composition and surface condition as well as the size distribution of the particles can affect the order of the particles in the monolayer.

**Key words** Monolayer · Gold nanoparticles · Silver · Rare-earth carbonate · Electrophoretic deposition

## Introduction

The properties of nanosized particles are different from usual materials due to their size. As the ability to assemble nanoparticles into well-defined 2D or 3D spatial configurations produces interesting properties, such as new collective physical behavior [1], the development of a general method for the production of such quantum crystals is a major challenge for future research. Several approaches, such as self-organization [2–7] and Langmuir–Blodgett (LB) techniques [8], have been used in order to obtain 2D and 3D structures. Such structures may be useful models for electron transport across grain boundaries in metals and may be used in producing optical gratings, optical filters, and data storage and microelectronic devices [4, 9, 10].

The self-organization of nanoparticles requires a hard-sphere repulsion, a controlled size distribution, and an inherent van der Waals attraction between the particles and the dispersion forces. Polydispersion in the particle size prevents the construction of such well-defined 2D or 3D structures and an appropriate surface passivation is required. The limitation of this method is that when the colloidal sols are allowed to dry on the grids, solvent evaporation tends to create circular voids, from which the particles are excluded. Another problem is that a large number of water-soluble colloids tend to aggregate instead of forming ordered 2D structures after the solvent evaporates. To avoid this problem, external forces are employed, such as LB techniques [8] and the electrophoretic deposition (EPD) method [11–14]. EPD of nanoparticles was first used by Giersig and Mulvaney [11, 12] to prepare ordered monolayers of gold nanoparticles. Prior to that, this method had only been used to produce 2D and 3D ordered structures of latex particles, such as polystyrene and silica [13, 14]. The advantage of the EPD method is that it requires no special surface passivation on the colloidal particles and it can be controlled conveniently by altering the applied field strength. It has been put forward by some researchers that the EPD method can be developed into a general method to prepare 2D and 3D ordered structures of nanoparticles by means of using sols that maintain colloidal stable on the electrode/sol interface; however, this conclusion is only based on the work done on micrometer-sized polystyrene, silica particles, and nanometer-sized gold particles and it requires further evidence. Giersig and Mulvaney investigated the effect of deposition time and surface passivation of gold particles on the deposition structure, but not how to

control the deposition structure. Here, we present a modified EPD method, whereby the order of the structures formed on a 20-nm amorphous carbon film adhering to the microscope grid is improved, with a better control over the structures formed. Two-dimensional structures of silver and rare-earth carbonate nanoparticles are prepared, providing further evidence for the conclusion mentioned previously.

## Experimental

Gold nanoparticles were prepared according to the method of Turkevich et al. [15] by using citrate to reduce $AuCl_4^-$. The mean particle size, as determined by electron microscopic analysis, was 10.6 nm. The standard deviation was 9.4%. Colloidal silver was prepared by reducing $AgNO_3$ with tannic acid. $AgNO_3$ solution 4 ml 0.1 mol $dm^{-3}$ was added to 100 ml distilled water and 1–2 ml 1% tannic acid solution was added to the mixture. The mixture was then heated to 70–80 °C and then 2 ml 1% $Na_2CO_3$ solution was added dropwise with constant stirring. The rare-earth carbonate sols were prepared according to the following procedures [16]. A certain volume of 0.01 mol $dm^{-3}$ $Gd(NO_3)_3$, or $Sm(NO_3)_3$, and an equal volume of 3 mol $dm^{-3}$ urea were fully mixed. The solution was heated to 85–90 °C in a water bath. Aging continued for 10 min after the first appearance of a "bluish" tint in the clear solution and a milk white sol formed. Then, the sol was cooled in an ice–water bath for 5 min.

The conductivity of the sols obtained was then decreased to less than 8 $\mu$S $cm^{-1}$ by dialysis. Electrophoresis was carried out using the method of Giersig and Mulvaney [11, 12]. A PAR M173 potentiostat and a PAR M175 function generator were used to generate the applied voltage. A 20-nm amorphous carbon film which adhered to the microscope grid was used as the support. The carbon film was made using a Hitachi HUS-5GB high-vacuum evaporator. The vacuum was maintained at $10^{-5}$ torr, the current was 35 A, and the deposition time was 5 min. A freshly cleaved mica sheet was used as the deposition support. The distance between the mica sheet and the carbon rod was 14 cm. After deposition, the carbon film was stripped from the mica sheet in an acetone/aqueous solution ($V_{acetone}$:$V_{water}$ = 1:9). Then the copper microscope grid was used to dredge up the stripped carbon film from the solution. Because the hydrophilic carbon film surface tended to be hydrophobic with time, electrophoresis was started within 1 day after vacuum deposition in order to get repeatable results. The UV–vis spectrum was recorded using a Shimadzu UV-240 spectrophotometer. The lattices were examined using a Hitachi H-800 transmission electron microscope operated at 100 kV. The size distributions of the particles were measured from enlarged photographs of the transmission electron microscope images.

## Results and discussion

### Electrophoresis of gold nanoparticles

Nanosized gold colloids show a very intense surface plasma absorption band in the visible range. Early work by Turkevich et al. [17] showed that particle sizes between 7.5 and 33 nm would correspond to a spectrum with a peak at 522 nm. The UV–vis spectrum of our Au nanoparticle sol is given in Fig. 1. Examination of the spectrum shows a little absorption at long wavelengths; however, at shorter wavelengths the absorption rises to a maximum at 518 nm, falling to a value of about two-thirds of the maximum at 450 nm, and finally rising steadily in the UV region to the limit of the measurements at 200 nm.

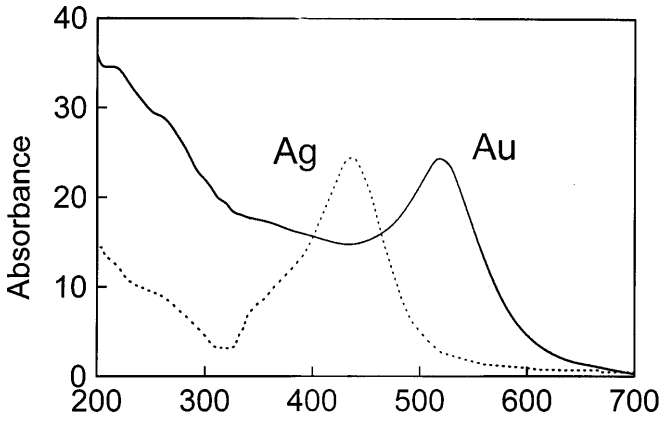


**Fig. 1** UV–vis spectra of Au sol particles (—) and Ag sol nanoparticles (- - -)

The deposition structures of gold nanoparticles obtained under 100, 500 and 1000 mV $cm^{-1}$ electric field strength for 300 s are shown in Fig. 2; the temperature is 20 °C. The electron micrograph easily fails to give the average information, so it is difficult to discuss the slight difference in the particle deposition density and ordered structure. In this work, the same experiment was carried out at least ten times and the averaged results are reported here. The deposited structure obtained under 100 mV $cm^{-1}$ contains only a few separated 2D structures formed by several particles, no large area of an ordered layer was found. When the field strength rose to 500 mV $cm^{-1}$, large areas of 2D ordered structures were observed. These structures were formed by connected rafts, each raft contained many ordered domains, and the particles in the domains were packed orderly and formed densely packed structures. A few voids were found in the rafts; possibly, this could be attributed to the evaporation of solvent. When the field strength reached 1000 mV $cm^{-1}$, ordered structures formed by gold particles were apparently more densely packed than those formed under 500 mV $cm^{-1}$ field strength, the size of the rafts increased, each domain contained more particles, and the number of randomly packed particles between ordered domains decreased. Under 500 and 1000 mV $cm^{-1}$ field strength, the coverage of 2D structures formed by the gold particles reached above 80% in the rafts; this was much higher than that obtained by the self-assembly method [18].

From the enlarged photograph in Fig. 2b calculation shows that the mean diameter of the Au particles is 10.6 nm and that the size deviation is 9.4%. The histogram of the size distribution is shown in the insert of Fig. 2b.

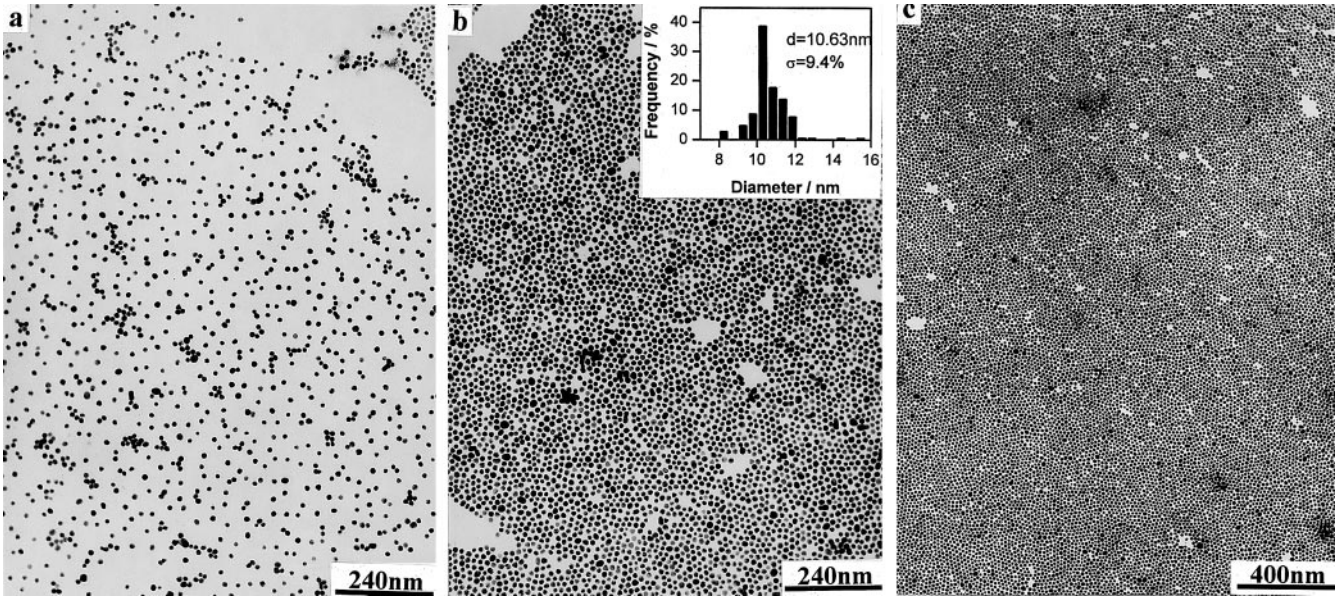


**Fig. 2a–c** Transmission electron microscope (*TEM*) images of Au nanoparticles on carbon-coated copper grids formed by electrophoresis with different direct current voltages. The deposition time is 5 min, the temperature is 20 °C. **a** 100 mV $cm^{-1}$; **b** 500 mV $cm^{-1}$; **c** 1000 mV $cm^{-1}$. *Insert* in **b**: the size distribution of Au nanoparticles

The viscosity of the solution and the thermodynamic speed of the particles varied with temperature; these could affect the speed of particles moving to the electrode. The 2D structures deposited at 32 °C under 500 mV $cm^{-1}$ field strength for 300 s are shown in Fig. 3. By comparing Fig. 3a with Fig. 1b, it is apparent that with the increase in temperature the area of the rafts of the ordered structure decreased, more voids appeared in the layer, and coverage of the monolayer decreased.

Typical structures obtained by the application of different frequency square-wave pulses are shown in Fig. 3b and c. The tendency for the crystalline domain size to increase with the frequency of the pulse is apparent. In the structure obtained under 500 mV $cm^{-1}$ direct current (d.c.) field strength (Fig. 2b), the domain size is small, many clusters containing only several particles could be found, and between the domains some

**Fig. 3a–c** TEM images of Au nanoparticles on carbon-coated copper grids formed by electrophoresis. **a** 500 mV $cm^{-1}$, 32 °C, 5 min; **b** 0–500 mV $cm^{-1}$ square-wave pulse, the pulse length is 1 s, the deposition time 10 min, 20 °C; **c** 0–500 mV $cm^{-1}$ square-wave pulse, the pulse length is 0.1 s, the deposition time 10 min, 20 °C

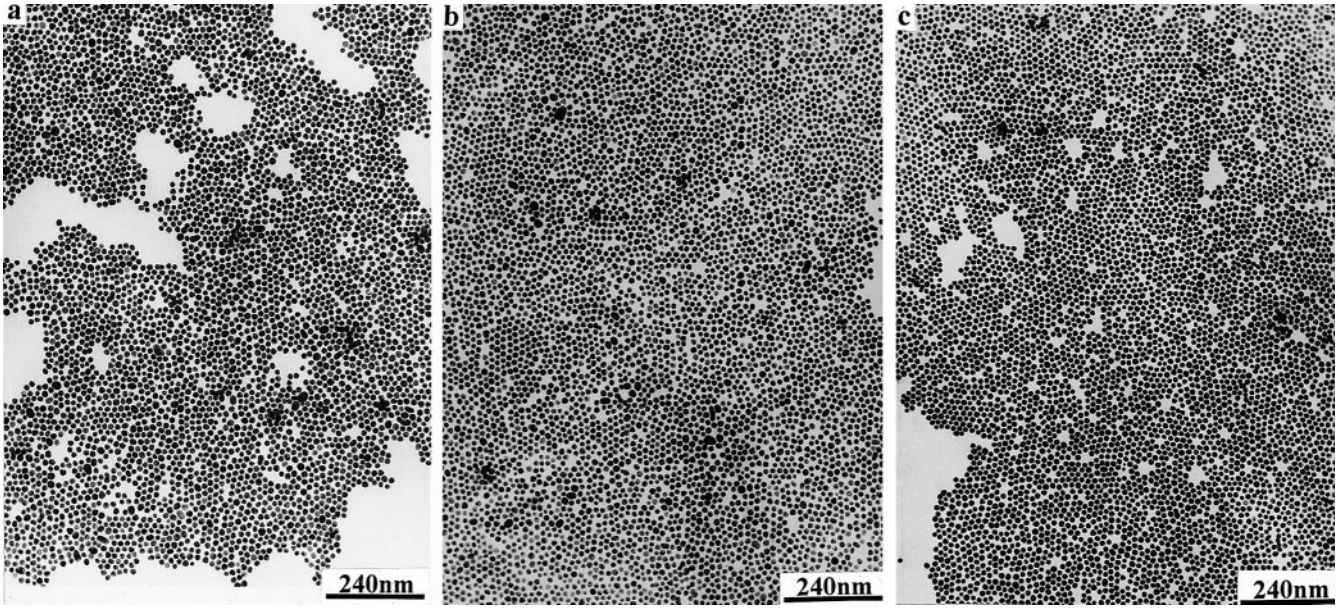

randomly packed individual particles are inserted; however, in Fig. 3b and c, the domain size is observed to increase with increased pulse wave frequency and the number of small clusters and randomly packed individual particles between the ordered domains is reduced.

When the pulse length was longer than 5 s, the effect of the pulse was not clear; it is very similar to the effect of d.c. voltage; however, when the pulse length was below 1 s, the effect became apparent. As ordered monolayer formation was dominant in the EPD procedure, it can be assumed that the formation of an ordered monolayer would give the largest Gibbs energy gain to the particles. Under d.c. voltage, the lateral attraction existed during the whole EPD procedure due to electrophoresis and the possibility of particle movements was limited after adsorption on the grid. With a square-wave pulse, during the relaxation time, the crystal structures formed under the electric field began to melt due to Brownian motion. In this way particles not so orderly packed were able to move to a better location, thereby achieving the largest free-energy gain and forming more ordered structures. During this procedure, a certain number of particles previously in the second layer would be transferred to the first layer. As the procedure was repeated a higher order was achieved and the number of particles in the second layer was reduced. The shorter the pulse length, the more apparent the effect, as shown in Fig. 3b and c.

## Assembly of silver particles

The UV absorption spectrum of the silver particles is shown in Fig. 1b. It is in good accordance with that in Ref. [19]. The absorption peak near 400 nm was attributed to the plasma excitation of the surface of the silver particles. Mie [19] and Wang et al. [20] have reported that the position of the absorption depends on the size of the metal particles: the peak moves toward long wavelengths as the size of the particle increases. The absorption peak near 400 nm was formed by two or three connected peaks; this indicates that the diameter of the silver particles was not homogeneous, and transmission electron microscopy confirmed this conclusion.

Under an applied d.c. electric field, the silver particles could also form 2D ordered structures on the electrode (Fig. 4a). From Fig. 4a the size distributions of the Ag particles were measured: the diameter of the silver particles was 8.1 nm and the size deviation was 29.4%, which was greater than that of the gold particles. The histogram of the size distribution is shown in the insert of Fig. 4a. Though the size deviation of the silver particles was greater than that of the gold particles, the silver particles could also form densely packed structures; however, the particles were not so orderly packed as the gold particles and the coverage was lower. The deposition structures formed by the silver particles were mainly 2D when the field strength ranged from 250 to 750 mV $cm^{-1}$. It could be observed that particles having similar diameter tended to pack together to form a more orderly packed area. This is the phenomenon termed selection of diameter.

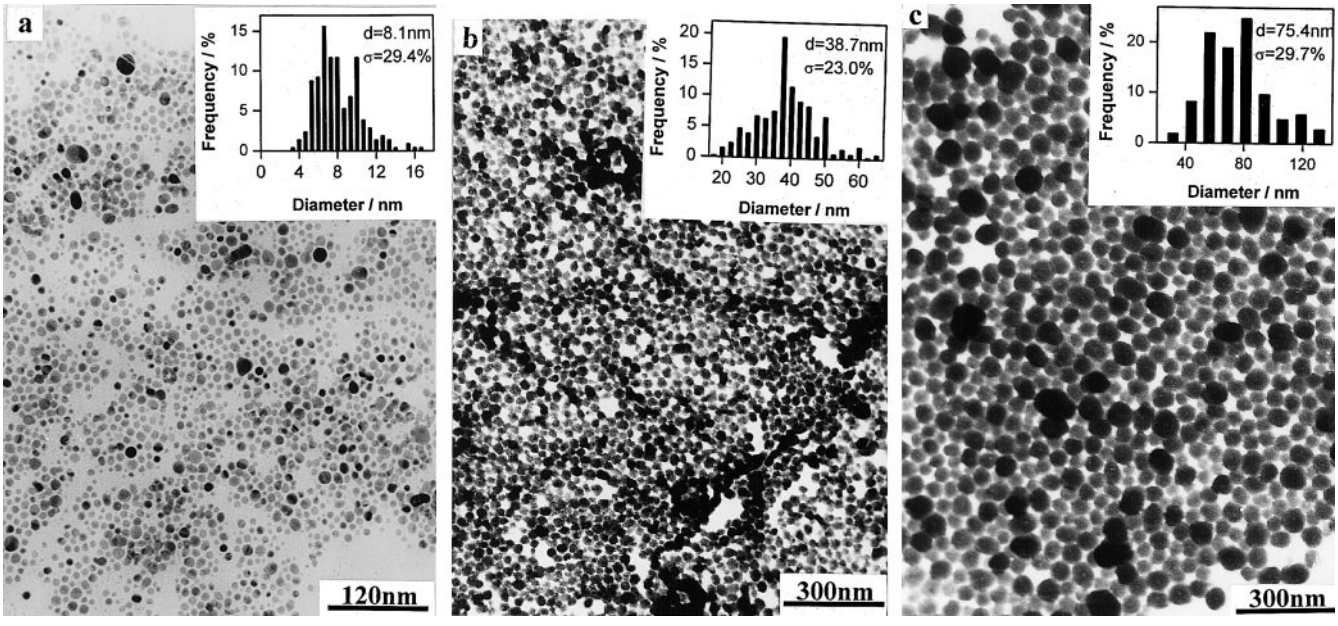


**Fig. 4** TEM images of **a** Ag nanoparticles, 500 mV $cm^{-1}$, 20 °C, 5 min, **b** $Gd_2(CO_3)_3$ nanoparticles, 500 mV $cm^{-1}$, 20 °C, 5 min, and **c** $Sm_2(CO_3)_3$ nanoparticles, 0–500 mV $cm^{-1}$ square-wave pulse, the pulse length is 10 ms, the deposition time 10 min, 20 °C on carbon-coated copper grids formed by electrophoresis. *Inserts*: the size distribution of the nanoparticles

Assembly of nanoparticles of rare-earth carbonates

In the later part of the twentieth century, a large amount of work was carried out on rare-earth elements. Due to their unique properties, these elements were applied in the fields of quantum electronics, medical science, and catalysis. In this work we prepared monolayers of $Gd_2(CO_3)_3$ and $Sm_2(CO_3)_3$ nanoparticles. These monolayers may be useful in the study of the catalytic properties of rare-earth elements.

The structure formed by $Gd_2(CO_3)_3$ nanoparticles deposited on the electrode is shown in Fig. 4b. When the grid was just immersed in the sol, no electric field was applied; only separated islands formed by several randomly packed particles were obtained, like dispersion-controlled coagulation of the gold sol. When a 500 mV $cm^{-1}$ d.c. electric field was applied, a large area of 2D structures could be observed; the particles in the layer were relatively densely packed. The layer was closer and no tears existed, only a few voids were present and these could be attributed to solvent evaporation. The area containing a multilayer was very small.

When just a drop of sol was dropped on the grid and the sample was allowed to dry in air, $Sm_2(CO_3)_3$ particles only formed islands similar to those of the $Gd_2(CO_3)_3$ particles; however, when a square-wave pulse was applied, a large-area monolayer could be observed on the grid. The particles were very densely packed and no multilayer could be observed (Fig. 4c).

The size distributions of the $Gd_2(CO_3)_3$ particles and the $Sm_2(CO_3)_3$ particles are shown in the inserts of Fig. 4b and c. The diameter of the $Gd_2(CO_3)_3$ particles was 38.7 nm and the size deviation was 23.0%. The diameter of the $Sm_2(CO_3)_3$ particles was 75.4 nm and the size deviation was 29.7%.

In the aspect of size distribution, the deviations of the $Gd_2(CO_3)_3$, the $Sm_2(CO_3)_3$, and the silver particles were similar, but in the deposited structure, silver particles and $Sm_2(CO_3)_3$ particles are apparently more orderly packed than $Gd_2(CO_3)_3$ particles. These results indicate that size distribution is only one element that has an effect on the order of the deposited structure and that the composition and surface condition of the particles have effects on the order of the deposited structure which are not negligible.

## Conclusion

Higher field strength can result in more orderly packed structures and higher coverage in the 2D structure and this may be caused by stronger attractive forces between particles under higher field strength. Rising temperature leads to a decrease in the monolayer area and coverage; however, square-wave pulses can improve the order of gold particles in the deposition structure and restrain the formation of a multilayer. Silver and rare-earth carbonate particles can also form 2D structures under applied electric fields, the difference is that these particles are not so orderly packed as gold particles. The results indicate that the ordering of nanoparticles under an electric field is a general phenomenon for colloidal sols and maintains colloidal stable on the interface. Moreover, the composition and surface condition as well as the size distribution of the particles can affect the order of the particles in the monolayer.

**Acknowledgements** This project is supported by the China Climbing Program no.97021107 and the State Key Laboratory for Corrosion and Protection, Academic Sinica.

## References

1. Heitmam D, Kotthaus JP (1993) Phys Today 56
2. Denkov ND, Velev OD, Kralchevaky PA, Ivanov IB, Yoshimura H, Nagayama K (1992) Langmuir 8:3183
3. Hayashi S, Kumamoto Y, Suzuki T, Hirai T (1991) J Colloid Interface Sci 144:538
4. Yosimura H, Matsumoto M, Endo S, Nagayama K (1990) Ultramicroscopy 32:265
5. Schatzel K, Ackerson BJ (1992) Phys Rev Lett 68:337
6. Van Megan W, Underwood SM (1993) Nature 362:616
7. Okubo T (1994) Langmuir 10:1695
8. James RH, Charles MK, Daniel VL (1997) J Phys Chem B 101:189
9. Xia Y, Kim E, Mrksich M, Whitesides GM (1996) Chem Mater 8:601
10. Kumar A, Whitesides GM (1994) Science 163:60
11. Giersig M, Mulvaney P (1993) J Phys Chem 97:6334
12. Giersig M, Mulvaney P (1993) Langmuir 9:3408
13. Yeh Syun-Ru, Michael S, Boris IS (1997) Nature 386:57
14. Trau M, Saville DA, Aksay IA (1996) Science 272:706
15. Enustun BV, Turkevich J (1963) J Am Chem Soc 85:3317
16. Soedelet D, Akinc M (1988) J Colloid Interface Sci 122:47
17. Turkevich J, Garton G, Stevenson PC (1954) J Colloid Sci Suppl 1:26
18. Colvin VL, Alivisatos AP, Tobin JG (1991) Phys Rev Lett 66:2786
19. Mie G (1908) Ann Phys 25:377
20. Wang DS, Kerker M, Shew H (1990) Appl Opt 19:2135